ARTICLE

Study on the Mechanism of Dispersion of Nano-Reinforcing Agents in Composites on Their Mechanical Properties and Thermal Stability

Gang Wang [1,*]

[1] School of Chemistry and Chemical Engineering, South China University of Technology, Guangzhou, 510000

Abstract

In this paper, the main materials and formulations for the experiment are selected, and the instruments and equipment required for testing are determined. According to the method of staple fiber orientation, the preparation of aramid staple fiber (nano-enhancer) is completed. The characterization methods of dispersion, thermal stability and mechanical properties are constructed, and the research data are synthesized to explore the mechanism of the dispersion of nano-reinforcing agent on the material properties. It can be concluded that the dispersion coefficient has a positive growth relationship with the hardness, tensile strength, Young's modulus, and elongation; moreover, the increase in the dispersion coefficient of the nano-reinforcing agent results in a decrease in the thermal cracking temperature of the composites, and the amount of residual carbon of the nano-reinforcing agent at 800°C is 2.44%, i.e., dispersibility catalyzes the thermal stability of the composites. This study reveals the mechanism of the dispersion of nano-reinforcement on its mechanical properties and thermal stability, which is an important guiding value for the development of composite materials and academic research.

Keywords: dispersibility, thermal stability, mechanical properties, nano-reinforcement, composites

Citation
Gang Wang (2024). Study on the Mechanism of Dispersion of Nano-Reinforcing Agents in Composites on Their Mechanical Properties and Thermal Stability . Mari Papel Y Corrugado, 2024(1), 14–23.

Submitted: 03 January 2024
Accepted: 15 March 2024
Published: 30 April 2024

Vol. 2024, **No.** 1, 2024.

***Corresponding author:**
✉ Gang Wang
211Mislywang@yahoo.com

1 Introduction

The materials industry is an important pillar of modern manufacturing industry, which is of great significance to the development of economy and society and the enhancement of comprehensive national power. The development of modern technology and the growth of application needs put forward higher and higher requirements for the development of materials science. Since most of the composite materials have the disadvantages of low hardness, insufficient rigidity, non-high temperature resistance, easy aging, etc., chemical modification, blend modification, aggregation state structure modulation and filling enhancement have been utilized to further improve the performance of polymer materials and expand the applications of composite materials [1–4]. Compared with traditional fillers, nano-fillers have quantum size effect and high specific surface area, and a lower filling amount can greatly improve the mechanical, electrical, thermal, magnetic, optical and other properties of composite materials, which has become a hot spot of the current domestic and international research on composite material modification technology [5–8].

The biggest problem plaguing researchers in the use of nanoenhancers is that they must ensure that they can be uniformly dispersed in composites [9, 10]. If the dispersion of nano-enhancers in composites is poor, they are prone to form non-uniform composites, which form inhomogeneous multiphase systems at different

locations within the composites, leading to the creation of weak regions with no or too little material locally [11–14]. Then the addition of nano-reinforcers can only be counterproductive, reducing the intrinsic quality of the whole composite material, artificially increasing the defects of the composite material, and decreasing the mechanical properties and service life [15–18]. In addition, if the nano-reinforcing agent substances produce phenomena such as adhesion and clustering, the mechanical properties and thermal stability of the composites will have a great negative impact [19, 20]. Therefore, it is fundamental to require the nano-enhancers to improve the dispersion of the substance components by mechanical stirring in the use of nano-enhancers on the one hand, and on the other hand, to make the nano-enhancers have good dispersion properties by special surface treatment [21, 22].

In this paper, the research program is designed to purchase the main raw materials and test formulas necessary for the research experiments from suppliers all over the world, and in order to guarantee the smooth implementation of the experiments, it is also necessary to further determine the appropriate experimental apparatus and data measurement equipment. After completing the above preparatory work, now formally start the preparation of experimental specimens, based on the knowledge of physical theory and chemical theory, respectively, to derive the dispersibility of the research samples, thermal stability, mechanical properties of the formula, through the experimental apparatus and equipment to obtain experimental data. Finally, the research data are used as a starting point to compare the performance differences of composites under different conditions of nano-enhancer dispersion coefficients.

2 Materials and Methods

2.1 Main raw materials and formulations

2.1.1 Main raw materials

Other materials used in the test are shown in Table 1. Natural rubber is used to produce a first-class smoke rubber from Thailand, the manufacturer Thailand Tongtai Standard Rubber Company, product model: STR20. pre-dispersed aramid staple fiber, aramid staple fiber as nano enhancement agent. Two products were selected for this study, one of which is the aramid staple fiber pulp product EE produced by DuPont applying its patented technology, the content of the pulp in this product is about 22.3%, and the rest is natural rubber. The other product is Teijin's aramid staple fiber pre-dispersed patented product SULRON6000, the product's fiber content of 45%, the remaining 55% of the sulfide and hard acid. The length of the staple fiber is about 11mm, the diameter is 16μm, and the L/D ratio is about 688.

2.1.2 Test formulations

The basic formulation of natural rubber with aramid staple fiber (nano enhancer) is shown in Table 2, and the basic formulation of natural rubber with aramid staple fiber (nano enhancer) is shown in Table 3. The basic formula is one of the forms of expression of the formula, is a form of expression of the formula to describe the relative amount of components in the formula by mass parts, in the form of expression of the raw rubber is generally set as 100.

2.2 Main instruments and equipment

The main instruments and equipment used in this subject are shown in Table 4. It can be seen that the main equipment and devices used in this subject are Torque Rheometer, Test Small Dense Kneader, 160MM Open Kneader, Flat Plate Vulcanizing Machine, Standard Dumbbell Cutter, Standard Trouser Shape Tear Cutter, Thermal Oxygen Aging Test Chamber, Instrument Name, Material Tensile Tester, Akron Abrasion Tester, Hardness Tester, Fluorescence Microscope, Scanning Electron Microscope, and Dynamic Mechanical Properties Analysis.

2.3 Sample Preparation

2.3.1 Staple fiber orientation methods

In order to solve the problem of orientation of aramid staple fibers (nano-reinforcements), the sample making method was specially designed. The specimens of mechanical properties were stacked by four layers of calendered specimens before mold vulcanization, and the calendering direction of the four layers of specimens was perpendicular to the adjacent specimens and parallel to the specimens of the interlayer. Curing specimen mold is square, four layers of stacked specimens are also square, stacked specimens are placed in the center of the mold to ensure that the elongation in both directions during molding is the same. This treatment makes the specimen test conditions closer to the actual use of tire rubber in the force situation.

2.3.2 Test preparation process

Conversion from the basic formula to the formula for testing. The mixing equipment for the basic formula

Categories	Name	Specification	Producer	Remark
Reinforcing agent	Carbon black	N220	Tianjin dolphin	
	White carbon black	VN3	Degussa (Germany)	Factory production in Taiwan
Anti-aging agent	Antiozone agent	4020	Lanxess (Bayer)	Factory production in India
	Antioxidant	RD	Tianjin Maofeng	
	Protective wax	RP-3	Fushun Petrochemical Research Institute	
Processing aid	Aromatic oil	BDA-2	Dagang Petrochemical (Sinopec)	
Activator	Zinc oxide	ZnO	Haixing in Hebei Province	Indirect method 99.7%
	Stearic acid	800	Zibo Boxin	
Tackifier	Carbon five petroleum resin	PRC-100	Jingjiang Jiangyuan Chemical	
Vulcanizing agent	Sulfur powder	S_8	Xinji, Hebei	
Accelerator	Accelerator	TBBS	LANXess (Bayer)	
Antiscorch agent	Antiscorch agent	CTP	Shandong Yanggu Huatai	

Table 1. Other materials used in the experiment

Name	00	01	02	03	04	05	06	07	08	09	10
STR20	100	100	100	100	100	100	100	100	100	100	100
EE	0	1	2	3	4	5	6	7	8	9	10
ZnO	3	3	3	3	3	3	3	3	3	3	3
St.A	2	2	2	2	2	2	2	2	2	2	2
T	2	2	2	2	2	2	2	2	2	2	2
S	2	2	2	2	2	2	2	2	2	2	2
NOBS	1	1	1	1	1	1	1	1	1	1	1
Total	110	111	112	113	114	115	116	117	118	119	120

Table 2. The basic formula of natural rubber and aramid pulp

Name	00	11	12	13	14	15	16	17	18	19	20
STR20	100	100	100	100	100	100	100	100	100	100	100
Sulron3000	0	1	2	3	4	5	6	7	8	9	10
ZnO	3	3	3	3	3	3	3	3	3	3	3
St.A	2	2	2	2	2	2	2	2	2	2	2
T	2	2	2	2	2	2	2	2	2	2	2
S	2	2	2	2	2	2	2	2	2	2	2
NOBS	1	1	1	1	1	1	1	1	1	1	1
Total	110	111	112	113	114	115	116	117	118	119	120

Table 3. The basic formula of natural rubber and aramidon short fiber

Device name	Type	Producer
Torque rheometer	XSS-30	Shanghai Kechuang rubber machinery equipment· Co., LTD. (formerly Shanghai Light machine mouldTool factory)
Small test mixer		Huagong Baichuan Technology Co., LTD
160MM open mill	160mm	Britain
Plate vulcanizer	400 * 400 plate vulcanizing machine (steam heating)	Qingdao Institute of Chemical Engineering machinery factory
Standard dumbbell cutter	Type 2	Beijing rubber Industry Design and Research Institute
Standard trouser tear cutter		Beijing rubber Industry Design and Research Institute
Hot oxygen aging test chamber	401A Type	Shanghai Chemical Machinery Plant No. 4
Instrument name	Model number	Manufacturer
Material tensile testing machine	TENSOMETER2000	Alpha corporation
Akron abrasion testing machine	MH-74	Shanghai Chemical Machinery Plant No. 4
Durometer	Sauer Type A	German
Fluorescence microscope	TE2000-U	Nikon Corporation of Japan
Scanning electron microscope	QUANTA200	American FEI Corporation.
Dynamic mechanical properties analysis	DMA242	DMA242

Table 4. The main experiment and the equipment model and the production factory

is a torque rheometer, the rotor is in the form of a three-pronged shape, and the working volume is 50 ml. The specific gravity of the rubber material is about 0.95 g/cm³ or so. After the field test on the No. 5 sample, 45g sample around, the upper pressure weight pressed down the length of time is moderate (about 3min), so 45g was selected as the best working volume. The dosing sequence and operation points of formula 00 to 20 mixing are shown in Table 5, and the dosing sequence and operation points of formula 00 to 20 mixing are shown in Table 6.

The mixing process was as follows: firstly, the temperature of the torque rheometer was raised to 50°C, and the test could be carried out only after the temperature was stabilized. All materials were weighed by balance and the data were accurate to 0.01 g. The rotor speed was set to 20 rpm. The weight of the pressurized weight was 5 kg.Preparation of samples for fluorescence microscopy. Firstly, the rubber was vulcanized into 6 × 15 × 50 mm specimens on a plate vulcanizing machine, and the vulcanization conditions were 152°C × 20 min, and the specimens were not processed before being loaded into the mold. After vulcanization, the observation surface of the specimen was gently sanded with a 200-mesh grinding wheel until the surface had a layer of very uniform and fine abrasive marks.

Preparation of samples for fluorescence microscopy. Firstly, the rubber was vulcanized into 6 × 15 × 50 mm specimens on a plate vulcanizing machine, the vulcanization conditions were 152°C × 20 min, and the specimens were not processed before being loaded into the molds. After vulcanization, the observation surface of the specimen was lightly sanded with a 200-mesh grinding wheel until the surface had a layer of very uniform and fine abrasive marks. Tensile specimen and tear specimen preparation: the mixed rubber in the open refiner after 5 times of thin pass, the rubber under the 0.8mm film, and then in accordance with the above method: four layers for folding, each layer of film calendering direction are perpendicular to the adjacent layer of film calendering direction, and parallel to the calendering direction of the interlayer, the folded film is cut into a square, and the vulcanization of the mold has the same shape, the specimen should be placed in the center of the mold, to ensure that the rubber film is placed in the center of the mold, to ensure that the film is very uniform and fine. The test piece should be placed in the center of the mold as much as possible when loading the mold to ensure that the flow of the film is the same in all four directions. A deflation should be carried out when the mold is vulcanized and closed to ensure that the vulcanized sample is free of air bubbles and dense, and that the thickness of the sample is within the specified error range. The vulcanization conditions are 152°C and the vulcanization times are 40°C, 60°C and 100°C.

2.4 Experimental testing and characterization

2.4.1 Decentralization tests

Under an environmental condition of 20%∼75% relative humidity, aramid short fibers were added according to the mass ratio of adhesive:water:reinforcing agent of 1:0.5:0.1, and then 1.2 kg/m³, and stirred for 5 min, and an appropriate amount of the above composite mixture was added to a 100 mL beaker. Subsequently, the mix was equally divided into 5 equal masses, and the aramid short fibers and rubber were separated by pumping and filtering, and the residual mixture on the surface of the aramid short fibers was repeatedly cleaned with anhydrous ethanol and distilled water, and the aramid short fibers were taken out and placed in an oven for drying, and the mass of the aramid short fibers was weighed for each portion (to the accuracy of 0.0001 g). It can be expressed as:

$$S = \sqrt{\frac{\sum_{i=1}^{5} \left(X_i - \overline{X}\right)^2}{n-1}}, \tag{1}$$

$$\psi = \frac{S}{\overline{X}} \times 100\%, \tag{2}$$

$$\beta = e^{-\psi}, \tag{3}$$

where X_i is the mass of aramid staple fiber in a specimen, $\overline{X}$ is the average mass of aramid staple fiber in each specimen, S is the standard deviation, ψ is the coefficient of variation, and β is the coefficient of dispersion [23].

2.4.2 Thermal stability tests

In order to investigate the mechanism of the dispersion of nano-reinforcing agent (aramid staple fiber) in composites on its mechanical properties and thermal stability, here it is necessary to conduct thermal stability tests to obtain thermal stability data, and several testing methods are commonly used at present, including Thermogravimetric Analysis (TGA), Differential Scanning Calorimetry (DSC), Dynamic Thermo-mechanical Analysis (DMA), and Thermal Aging Performance Test [24, 25]. Here the properties of aramid staple fibers are considered, so differential scanning calorimetry (DSC) is used.

Step	Time	Controls	Remarks
1	0	"Add raw gum and pre-dispersed staple fiber or pulp.	
2	5	Press down on the weight	
3	120	Lifting weight	
4	126	Add other materials	
5	130	Press down on the weight.	
6	235	Lifting weight	
7	250	Press the weight	
8	360	Lifting weight	
9	365	Press down on the weight	
10	490	Raise the weight, open the engine room, and discharge the material	

Table 5. The order and operation points of the formula 00∼ 20 mixture

Step	Time	Controls	Remarks
1	0	Add a piece of glue	
2	8	Press down on the weight	
3	140	Lifting weight	
4	145	Press down on the weight	
5	230	Lifting weight	
6	240	Press down on the weight	
7	330	Raise the weight, open the engine room, discharge the material	

Table 6. The order and operation points of the formula 00∼ 20 mixture

Differential scanning calorimetry is a common method to measure the power difference between the sample and the reference as a function of temperature. When the temperature reaches the glass transition temperature, the heat capacity of polymer composites increases and needs to absorb external energy, which is shown as a turn of the baseline on the DSC curve. In this paper, the DSC test was carried out in a thermo-oxygen aging test chamber, scanning electron microscope, and the specific experimental conditions are as follows: the sample was placed in the oxygen aging test chamber, and the test was carried out in N_2 at a temperature increase rate of 10°C/min to ensure that the amount of the sample used in each test, the shape of the sample, the sample particle size and the rate of temperature increase were the same.

2.4.3 Mechanical performance tests

In order to study the mechanism of the dispersion of nano-reinforcement (aramid staple fiber) in composites on its mechanical properties and thermal stability, here the mechanical properties of composite nano-reinforcement (aramid staple fiber) need to be tested, and the test items mainly include hardness, room temperature tensile test, and high temperature tensile test [26, 27].

1. test

The hardness test in this paper uses the hardness tester mentioned above, and the basic principle of the test is shown in Figure 1. The stainless steel pressure needle at the indenter is pressed vertically into the surface of the sample under the action of the external load, until the pressure foot and the sample surface is completely adhered to, at this time, the tip of the pressure needle relative to the surface of the sample extends the length of the distance of L to L value to characterize the magnitude of the sample Shore hardness. Shore hardness and L value to meet the relationship (4):

$$HD \approx 100 - L/0.025. \tag{4}$$

In (4) Where HD is the hardness value of the reinforcing agent measured with a hardness tester. From the above equation, the larger L is, the lower HD is, and the smaller L is, the higher HD is. During the test, at least five test points should be selected for each sample, and each test point should be at least 6 mm apart, and the average value of the test results is taken as the final HD.

2. Room temperature tensile test

The tensile strength, elongation at break and Young's modulus of the nano-reinforcers (aramid staple fibers) were tested at room temperature

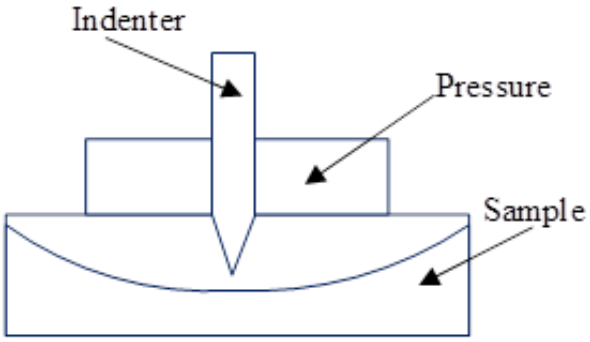

Figure 1. Test fundamentals

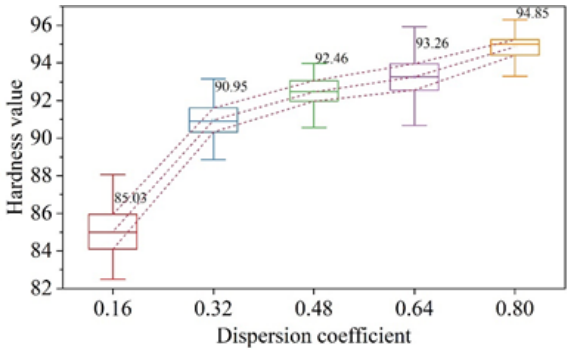

Figure 2. Dispersion on hardness

using a material tensile testing machine (as mentioned in subsection 2.2), and the load loading rate of the material tensile testing machine was 4 mm/min.

3. High temperature tensile test

The service temperature of the nano-enhancers (aramid staple fibers) prepared in this paper is generally lower than 500 ℃, so the tensile strength, elongation at break and Young's modulus of the nano-enhancers (aramid staple fibers) were tested using a material tensile testing machine at high temperatures of 150 ℃ and 400 ℃ respectively, and again, the loading rate was 4 mm/min.

3 Experimental results and discussion

3.1 Mechanisms of dispersion effects on mechanical properties

3.1.1 Analysis of the effect of dispersion on hardness

Dispersion on the hardness of the analysis shown in Figure 2, where the horizontal axis is the dispersion coefficient, the vertical axis is the hardness value. With the increase of the dispersion coefficient, the hardness value shows an upward trend, aramid staple fiber fiber is a material with high modulus, high strength, and because of its surface with small fibers make it and the resin must be supported in the friction material, so the hardness value is increased. However, when the dispersion coefficient continues to rise, the growth rate of its hardness value is relatively small, i.e., dispersion and hardness show a positive relationship. The dispersion coefficient can effectively improve the hardness value of the composite material, and it can have better hardness performance when facing the damage of external load.

3.1.2 Analysis of the effect of dispersion on room temperature stretching

Figure 3 demonstrates the results of the analysis of the effect of dispersion on room temperature tensile, where Figure 3(a) to (c) are the tensile strength, modulus, and elongation, respectively. The tensile strength, Young's modulus, and elongation of aramid staple fibers without the introduction of dispersion coefficient are 50 MPa, 700 MPa, and 11.27%, respectively. With the increase of the dispersion coefficient, the tensile strength, Young's modulus, and elongation of the aramid staple fiber fibers showed a significant increase. Notably, when the dispersion coefficient was 0.48, the tensile strength and Young's modulus of the composite film were 88.35 MPa, 859 MPa, and 14.95%, respectively, which were increased by 76.7%, 22.71%, and 32.65%, respectively, relative to those of the aramid staple fiber fiber fibers without the introduction of the dispersion coefficient. When the dispersion coefficient continued to increase, the tensile strength, Young's modulus, and elongation of aramid staple fibers fibers showed an increasing trend. The study shows that the effective stress transfer between polymer and nanoparticles is the main reason for the increase in tensile strength of nanocomposites The more dispersed the atomic structure is, the more conducive to the formation of effective interfacial bonding, which in turn effectively disperses the stress on the polymer in the process of stretching, and promotes the improvement of the mechanical properties of the composites.

3.1.3 Analysis of the effect of dispersion on high-temperature stretching

The results of the analysis of the effect of dispersion on high-temperature tensile are shown in Figure 4, where 4(a) to (c) are tensile strength, modulus, and elongation in order, and the values in the figure are T-values. Based on the data performance in the figure,

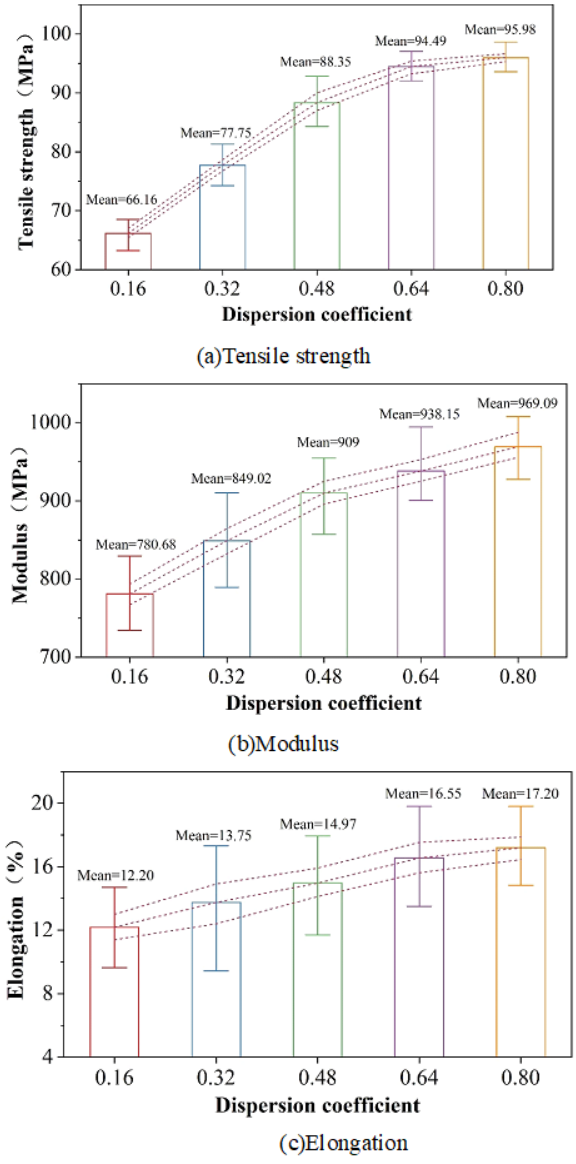

Figure 3. The dispersion is analyzed for the effect of room temperature

it can be seen that in terms of tensile strength with the increase of dispersion coefficient, the difference between the tensile strength of aramid staple fiber at 100℃ and 400℃ is getting smaller and smaller, and the P-value meets the standard condition of $P<0.05$, which indicates that there is a significant difference in tensile strength under the action of different dispersion coefficients, and modulus and elongation also satisfy the standard condition of $P<0.05$, here The modulus and elongation also satisfy the standard condition of $P<0.05$, which will not be repeated here. Overall, the tensile strength, modulus and elongation of aramid staple fibers are significantly different under different dispersion coefficients at 100℃ and 400℃, which greatly proves the role of dispersion in the promotion of high-temperature stretching of composites.

3.2 Mechanisms of dispersion effects on thermal stability

The thermal stability of composites is usually characterized by thermogravimetric analysis (TGA), which represents the loss of mass of a sample at a certain rate of temperature increase. Figure 5 shows the TGA curve (thermogravimetric analysis curve) and DTG curve (thermogravimetric differential curve) of the composites under nitrogen atmosphere, where 5(a)~(b) are the TGA curve and DTG curve, respectively. It can be seen in the figure that with the increase of the dispersion coefficient (0.16~0.80) of the nanoenhancer, the thermal cleavage of cellulose mainly occurs between 300~400 ℃, and the glycosidic and ether bonds inside the cellulose are broken, producing a large number of small molecules such as H_2O, CO, and moreover, the broken molecules rearrange their chemical bonds to obtain a series of intermediates, which are further decomposed to produce coke and volatile gases, resulting in a large amount of weight loss of the cellulose sample. The further decomposition produces coke and volatile gases, resulting in a large amount of weight loss of the cellulose sample, and the amount of residual carbon at 800°C is 2.44%. This indicates the catalytic effect of dispersion on the thermal stability of the composites. Meanwhile, due to the increase of dispersion coefficient, the thermal decomposition process of the composites also changed, as can be seen from the DTG curve, the initial decomposition temperature of the dispersion coefficient of 32.00% was about 155 ℃ earlier than that of the dispersion coefficient of 16.00%, respectively, and there were two main decomposition peaks, the first one appeared at 237 ℃, in which the carboxyl group in the molecular

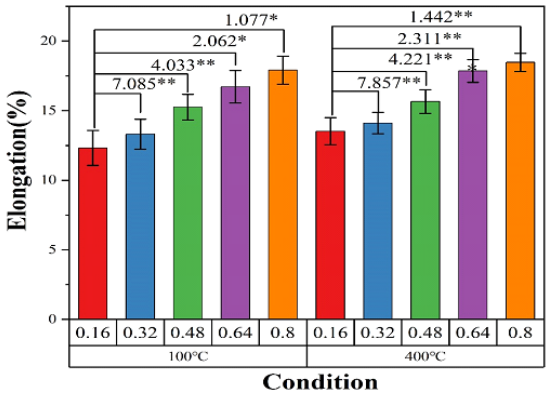

(c)Elongation

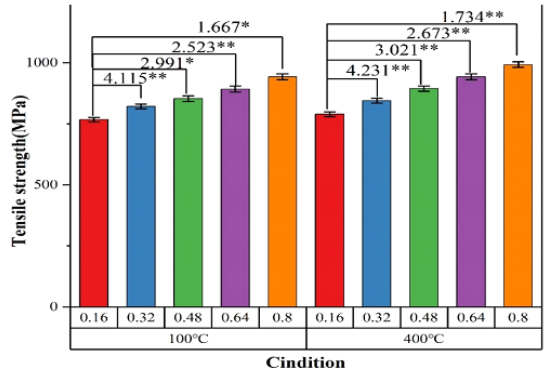

(b)Modulus

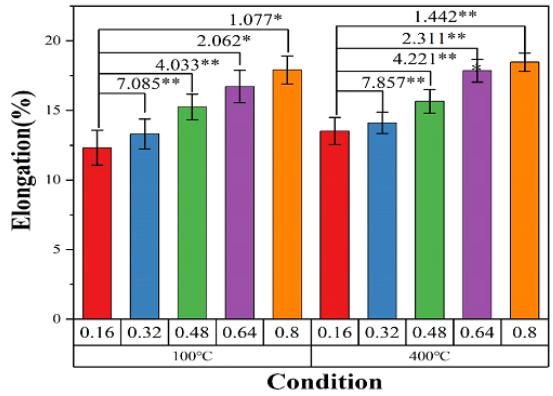

(c)Elongation

Figure 4. Dispersion of the results of the analysis of high temperature tensile influence

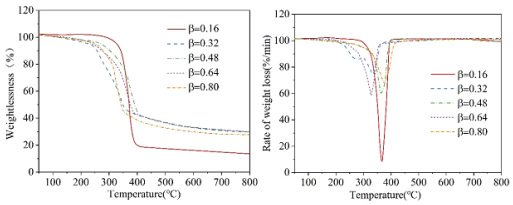

(a)TGA (b)DTG

Figure 5. TGA curve and DTG curve

structure of cellulose was decomposed by the thermal decomposition, decarboxylation reaction occurred, and the molecular chain was degraded thereafter. The first decomposition peak occurs at 237°C, at which the carboxyl group in the cellulose molecular structure is thermally decomposed and decarboxylation reaction occurs, and the molecular chain is degraded. Both major decomposition temperatures were greatly advanced than cellulose, and the thermal degradation rates of the two substances at the two major decomposition peaks were 4.21%·min^{-1} and 6.39%·min^{-1}, respectively, with values significantly lower than those of cellulose (20.9%·min^{-1}), and similarly, the dispersion coefficients of 48.00%, 64.00%, and 80.00% and 32.00% were similar, all possessing two main decomposition temperatures, with the highest amount of residual carbon for the dispersion coefficient of 64.00%.The increase in the dispersion coefficient was also effective in catalyzing the formation of carbon from cellulose.The presence of a part of carboxylic acid groups within the molecule led to the prolongation of the decarboxylation reaction time, which overlapped with the decomposition peaks of the generated residue, fully verifying that dispersibility has a catalytic effect on the thermal stability.

4 Conclusion

This paper identifies the raw materials, instruments, and equipment required for experimental analysis, prepares samples for experimental studies, and investigates the effect of dispersion of nano-reinforcing agents in composites on their mechanical properties and thermal stability. The main research results are as follows:

1. Under the condition of dispersion coefficient of nano-reinforcing agent, hardness, tensile strength, modulus and elongation have a positive effect relationship, and its analytical results have an important reference value for the improvement of composite material properties.
2. With the increase of the dispersion coefficient of

the nano-reinforcing agent, it leads to cause a large amount of weight loss of the nano-reinforcing agent, and the amount of residual carbon at 800℃ is 2.44%, which indicates that the dispersion has a catalytic effect on the thermal stability of the composite material itself, and in addition, the dispersion coefficient also leads to the change of the thermal cracking process of the composite material itself.

References

[1] Bello, S. A., Eleburuike, L. B., Adams, L. A., Kolawole, D. B., Kolawole, M. Y., Artur, E. K., & Iqbal, F. (2022). Emerging materials in polymer reinforcement. In Hybrid Polymeric Nanocomposites from Agricultural Waste (pp. 3-20). *CRC Press*.

[2] Tourani, N., Sagoe-Crentsil, K., & Duan, W. (2022). Strain-rate-dependent performance of cementitious nanocomposites: Nanosilica and the role of dispersion. *Cement and Concrete Research, 161*, 106966.

[3] Bakri, M. K. B., Rahman, M. R., Taib, S. N. L., Khui, P. L. N., Kakar, A., & Jayamani, E. (2021). Nano-reinforcement in sustainable polymer composites. In Advances in sustainable polymer composites (pp. 231-243). *Woodhead Publishing*.

[4] Banapurmath, N. R., Hallad, S. A., Hunashyal, A. M., Sajjan, A. M., Shettar, A. S., Ayachit, N. H., & Godi, M. T. (2019). Nanocomposites for structural and energy applications. Handbook of Ecomaterials; Martinez, LMT, Ed.; Springer International Publishing: *New York, NY, USA, 2*, 854-883.

[5] Norizan, M. N., Shazleen, S. S., Alias, A. H., Sabaruddin, F. A., Asyraf, M. R. M., Zainudin, E. S., ... & Norrrahim, M. N. F. (2022). Nanocellulose-based nanocomposites for sustainable applications: A review. *Nanomaterials, 12*(19), 3483.

[6] Ervina Efzan, M. N., & Siti Syazwani, N. (2018). A review on effect of nanoreinforcement on mechanical properties of polymer nanocomposites. *Solid State Phenomena, 280*, 284-293.

[7] Velmurugan, G., Shankar, V. S., Shree, S. G., Abarna, M., & Rupa, B. (2023). Review and Challenges of Green Polymer-Based Nanocomposite Materials. In International Conference on Sustainable Technologies and Advances in Automation, Aerospace and Robotics (pp. 613-624). *Springer*, Singapore.

[8] Hosseini, S. B. (2017). A review: Nanomaterials as a filler in natural fiber reinforced composites. *Journal of Natural Fibers, 14*(3), 311-325.

[9] Gao, Y., Jing, H. W., Chen, S. J., Du, M. R., Chen, W. Q., & Duan, W. H. (2019). Influence of ultrasonication on the dispersion and enhancing effect of graphene oxide–carbon nanotube hybrid nanoreinforcement in cementitious composite. Composites Part B: *Engineering, 164*, 45-53.

[10] Zamani, P., Alaei, M. H., da Silva, L. F., & Ghahremani-Moghadam, D. (2022). On the static and fatigue life of nano-reinforced Al-GFRP bonded joints under different dispersion treatments. *Fatigue & Fracture of Engineering Materials & Structures, 45*(4), 1088-1110.

[11] Yaghobian, M., & Whittleston, G. (2022). A critical review of carbon nanomaterials applied in cementitious composites–a focus on mechanical properties and dispersion techniques. *Alexandria Engineering Journal, 61*(5), 3417-3433.

[12] Khurram, A. A., Khan, A., Gul, I. H., & Subhani, T. (2018). Glass fiber epoxy matrix composites containing zero and two dimensional carbonaceous nanoreinforcements. *Polymer Composites, 39*(S4), E2056-E2063.

[13] Sadeghi, B., Cavaliere, P., & Sadeghian, B. (2023). Enhancing Strength and Toughness of Aluminum Laminated Composites through Hybrid Reinforcement Using Dispersion Engineering. *Journal of Composites Science, 7*(8), 332.

[14] Jiang, Z., Sevim, O., & Ozbulut, O. E. (2021). Mechanical properties of graphene nanoplatelets-reinforced concrete prepared with different dispersion techniques. *Construction and Building Materials, 303*, 124472.

[15] Akindoyo, J. O., Beg, M. D., Ghazali, S., Heim, H. P., & Feldmann, M. (2017). Effects of surface modification on dispersion, mechanical, thermal and dynamic mechanical properties of injection molded PLA-hydroxyapatite composites. Composites Part A: *Applied Science and Manufacturing, 103*, 96-105.

[16] Saba, N., Safwan, A., Sanyang, M. L., Mohammad, F., Pervaiz, M., Jawaid, M., ... & Sain, M. (2017). Thermal and dynamic mechanical properties of cellulose nanofibers reinforced epoxy composites. *International Journal of Biological Macromolecules, 102*, 822-828.

[17] Leong, K. Y., Rahman, M. R. A., & Gurunathan, B. A. (2019). Nano-enhanced phase change materials: A review of thermo-physical properties, applications and challenges. *Journal of Energy Storage, 21*, 18-31.

[18] Kumar, A., Sharma, K., & Dixit, A. R. (2019). A review of the mechanical and thermal properties of graphene and its hybrid polymer nanocomposites for structural applications. *Journal of Materials Science, 54*(8), 5992-6026.

[19] Fang, F., Ran, S., Fang, Z., Song, P., & Wang, H. (2019). Improved flame resistance and thermo-mechanical properties of epoxy resin nanocomposites from functionalized graphene oxide via self-assembly in water. Composites Part B: *Engineering, 165*, 406-416.

[20] Liu, Z., Li, J., & Liu, X. (2020). Novel functionalized BN nanosheets/epoxy composites with advanced thermal conductivity and mechanical properties. *ACS Applied Materials & Interfaces, 12*(5), 6503-6515.

[21] Emadinia, O., Vieira, M. T., & Vieira, M. F. (2018).

Effect of reinforcement type and dispersion on the hardening of sintered pure aluminium. *Metals, 8*(10), 786.

[22] Ismail, N. H., Akindoyo, J. O., & Mariatti, M. (2020). Solvent mediated dispersion of carbon nanotubes for glass fibre surface modification–Suspensions stability and its effects on mechanical, interlaminar and dynamic mechanical properties of modified glass fibre reinforced epoxy laminates. Composites Part A: *Applied Science and Manufacturing, 139*, 106091.

[23] Khaled, G., Bourouina-Bacha, S., Sabiri, N. E., Tighzert, H., Kechroud, N., & Bourouina, M. (2017). Simplified correlations of axial dispersion coefficient and porosity in a solid-liquid fluidized bed adsorber. *Experimental Thermal and Fluid Science, 88*, 317-325.

[24] Zamfirescu, C., Dincer, I., & Naterer, G. (2009). Performance evaluation of organic and titanium based working fluids for high-temperature heat pumps. *Thermochimica Acta, 496*(1-2), 18-25.

[25] Jung, H. S., Han, G. S., Park, N. G., & Ko, M. J. (2019). Flexible perovskite solar cells. *Joule, 3*(8), 1850-1880.

[26] Özel, T., & Karpat, Y. (2007). Identification of constitutive material model parameters for high-strain rate metal cutting conditions using evolutionary computational algorithms. *Materials and Manufacturing Processes, 22*(5), 659-667.

[27] Liang, Y., Cao, L., & Sang, S. (2023). Rock physical and mechanical properties test and comprehensive evaluation of the Longtan group in Well DH Can 1, Dahebian block, Guizhou Province. *International Journal of Oil, Gas and Coal Technology, 33*(3), 282-302.